Collecting high-order interactions in an effective pairwise intermolecular potential using the hydrated ion concept: The hydration of Cf3+

Elsa Galbis, Jorge Hernández-Cobos, Rafael R. Pappalardo, and Enrique Sánchez Marcos

Citation: The Journal of Chemical Physics **140**, 214104 (2014); doi: 10.1063/1.4879549
View online: http://dx.doi.org/10.1063/1.4879549
View Table of Contents: http://scitation.aip.org/content/aip/journal/jcp/140/21?ver=pdfcov
Published by the AIP Publishing

Collecting high-order interactions in an effective pairwise intermolecular potential using the hydrated ion concept: The hydration of Cf^{3+}

Elsa Galbis,[1] Jorge Hernández-Cobos,[2] Rafael R. Pappalardo,[1] and Enrique Sánchez Marcos[1,a)]
[1]*Departmento de Química Física, Universidad de Sevilla, 41012 Seville, Spain*
[2]*Instituto de Ciencias Físicas, UNAM, Apartado Postal 48-3, 62251 Cuernavaca, Mexico*

(Received 1 February 2014; accepted 7 May 2014; published online 3 June 2014)

This work proposes a new methodology to build interaction potentials between a highly charged metal cation and water molecules. These potentials, which can be used in classical computer simulations, have been fitted to reproduce quantum mechanical interaction energies (MP2 and BP86) for a wide range of $[M(H_2O)_n]^{m+}(H_2O)_\ell$ clusters (n going from 6 to 10 and ℓ from 0 to 18). A flexible and polarizable water shell model (Mobile Charge Density of Harmonic Oscillator) has been coupled to the cation-water potential. The simultaneous consideration of poly-hydrated clusters and the polarizability of the interacting particles allows the inclusion of the most important many-body effects in the new polarizable potential. Applications have been centered on the californium, Cf(III) the heaviest actinoid experimentally studied in solution. Two different strategies to select a set of about 2000 structures which are used for the potential building were checked. Monte Carlo simulations of Cf(III)+500 H_2O for three of the intermolecular potentials predict an aquaion structure with coordination number close to 8 and average $R_{Cf–O}$ in the range 2.43–2.48 Å, whereas the fourth one is closer to 9 with $R_{Cf–O} = 2.54$ Å. Simulated EXAFS spectra derived from the structural Monte Carlo distribution compares fairly well with the available experimental spectrum for the simulations bearing 8 water molecules. An angular distribution similar to that of a square antiprism is found for the octa-coordination. © *2014 AIP Publishing LLC*. [http://dx.doi.org/10.1063/1.4879549]

I. INTRODUCTION

The solution chemistry of actinides ions, or actinoids, is one of the most relevant domains related with some of the fundamental and practical fields of the nuclear technology, its environmental implications, and medical and engineering applications.[1,2] There are opening questions regarding the behavior of the heaviest actinoids known such as their experimental complexity, the lack of material, and their usual hazardness. These issues have precluded systematic studies along the series and knowledge of the physicochemical trends has not been completely fulfilled.[3] This framework of experimental restrictions makes theoretical methods particularly appropriate given that they offer a safe and inexpensive way to help in the achievement of a complete body of knowledge on this series.

The microscopic perspective provided by molecular methodologies usually facilitates a deeper understanding of the system and helps in proposing simple models. When dealing with solutions containing highly charged metal cations, it is widely accepted that statistical ingredients are needed together with a quantum-mechanical description of the inter- and intra-molecular interactions. *Ab initio* molecular dynamics techniques offer an appropriate tool to satisfy the demanding requirements for a reasonable description.[4] However, the highly computational resources demanded by this type of simulations limits the information obtained, because of small system sizes and short simulation times. This is the reason why sometimes the consideration of classical computer simulations appears as an alternative to obtain practical answers. In the context of classical simulations, a key-point is the use of reliable inter- and intra-molecular potentials.[5] There are many strategies proposed to solve this question going from operative empirical fitting to thorough decomposition of the interaction potentials in a series of many-body contributions and/or defining ways for updating molecular geometry and charge polarization of the particles defining the system.[6,7] A few actinide-water intermolecular potentials to be used in classical MD simulations have been reported in the bibliography. For Cm(III), Yang and Bursten[8] developed an intermolecular potential based on our hydrated ion model,[9–11] assuming a rigid ennea-coordination (nine-fold coordination) of the cation. Gagliardi *et al.*[12] developed a Cm(III)-H_2O intermolecular potential from high-level *ab initio* computation of this system where many-body interactions are included by means of the polarizable character of the water molecules and the ion, that are described by a perturbation theory-derived intermolecular potential (the NEMO approach).[13]

Atta-Fynn *et al.*[14] have developed another interaction potential including three-body corrections by fitting a ROHF potential energy surface. Spezia *et al.*[15] have proposed a polarizable interaction potential for the series of trivalent actinides, based on a previous systematic study carried out for the lanthanoids(III) series.[16] Taking as a reference the case of La(III),[17] an intermolecular potential is built based on *ab initio* interaction energies of the symmetric deformation of

a)Electronic mail: sanchez@us.es

$[La(H_2O)_8]^{3+}$. For the rest of the series is extended the approach assuming a systematic dependence of part of the functional form on tabulated ionic radii.

Midways strategies combine quantum-mechanical descriptions for the closest solute's environment and a classical representation for the rest of the solution, these are the hybrid QM/MM methods.[18,19]

It must be pointing out that in the absence of detailed physicochemical data for actinide series in aqueous solution, it has been usually assumed that the changes on the properties should be analogous to those observed for the Ln^{3+} series.[20,21] This experimental view has also been adopted by recent theoretical studies, when results derived for actinides and lanthanides trivalent cations in solution have been compared.[22,23] Thus, the systematic comparison between theoretical results obtained from actinide and lanthanides solutions, helps in getting insight into the experimental assumption on the use of Ln(III) ions as models of An(III) ions in the study of their chemistry in solution and solid state.

An intermolecular metal cation-water interaction model based on the old electrochemical concept of the hydrated ion was developed by our group some years ago. This model assumed that the entity interacting in aqueous solution is the hydrated ion, $[M(H_2O)_n]^{m+}$, rather than the bare cation M^{m+}. Its development implied the $[M(H_2O)_n]^{m+}$-H_2O interaction potential building, that intended to reproduce the *ab initio* interaction energies computed quantum-mechanically.[9–11] An additional intramolecular potential describing the internal dynamics of the aquaion was coupled to the intermolecular potential.[24] These potentials have been used in Monte Carlo and molecular dynamics simulations of some transition-metal cations showing the correct behavior of this model when compared to experiment.[25–29] The good agreement points out that the main many-body contributions are properly collected. For instance, the partial metal-water charge transfer and the strong polarization of the first-shell water molecules were pretty well described as they reproduced the QM calculations. Nevertheless, the model definition of an aqua ion leads to include two different types of water molecules in the simulation system, those belonging to the first-shell and those of the bulk. As a result the exchange of first-shell water molecules with outer hydration shells is precluded. Whereas in practice this is not a limitation when describing stable aqua ions, that is, hydrates having slow first-shell water molecule release kinetics,[30] it becomes a serious shortcoming when dealing with metal cations that exchange quickly water molecules in their first hydration shell.

In a previous communication on the Cf(III) hydration[31] we combined experimental EXAFS data on an aqueous solution of this actinoid with theoretical data coming from a Monte Carlo simulation which used a first proposal for a Cf–H_2O intermolecular potential. This was based on an extension of our hydrated ion model where the exchange of water molecules between the first hydration shell and the bulk was allowed. The development of such type of intermolecular potential involved the consideration of a large number of $[Cf(H_2O)_n]^{3+}$ structures, where both the number of water molecules and their relative orientations must change a lot in order to assure a good sampling of the collective interactions. This new methodology incorporates the explicit consideration of many-body contributions via the inclusion in the set of structures to be fitted of many symmetric and asymmetric geometries with a significant number of water molecules.

Because the first-principles nature of the fitting procedure of the classical Cf(III)-water potential developed, it was tested at the cluster level by comparing with quantum-mechanical computations, as well as by analyzing different properties derived from classical Monte Carlo simulations. Two potentials were obtained from MP2 or BP86 potential energy surfaces (PES). They gave a quite different coordination number, 8 vs. 9, as well as different Cf–O first-shell distances, $\Delta R = 0.1$ Å. The open question was whether it had been due to the different quantum-mechanical level, another uncontrolled factors, such as the functional form or PES sampling, or simply the discrepancy was due to the intrinsic methodological uncertainty associated to the intramolecular potential building, since there is not a unique way to define the set of clusters to be included in the fitting. To help in elucidating this question, the experimental EXAFS spectrum of a Cf(III) aqueous solution[31] was used as a reference for the simulated EXAFS spectrum which can be calculated from the structural information provided by the different Monte Carlo simulations. The present work proposes a refined methodology in order to build in a systematic way effective pair-potentials with high-order many-body contributions included both in an implicit average manner, and by the use of a polarizable model for the water molecule and the metal cation. The aim of this work is to provide a thorough analysis of the interaction potential building process, as well as the structural analysis of Cf(III) hydration.

II. METHODOLOGY

In order to carry out classical computer simulations of Cf(III) in water, the cation-water intermolecular potential must be built on the basis of a chosen water model. This section presents the previous hydrated ion model, on which the new potential model has been built, the upgrades introduced in the new potential, the quantum mechanical details of the PES used to fit the interaction potential, and the computer simulation conditions.

A. Extension of the HIW model

The Hydrated Ion-Water potential, HIW,[9–11] is suitable to describe highly charged metal cations in water, especially in such cases where the residence time of water molecules in the first solvation shell is longer than the simulation time.

The consideration of the cation with its first hydration shell as the species interacting in solution prevents the problems of charge transfer and electronic state crossing, which may appear when dealing with the *ab initio* computation of a set of ion-water structures where distances and relative orientations change a lot.[32] Differing from the simpler bare ion-water case (M^{m+}–H_2O), the hydrated cation is stable enough against the interaction with an additional water molecule ($[M(H_2O)_n]^{m+}$–H_2O) to avoid a charge transfer or an electronic state change with distance.

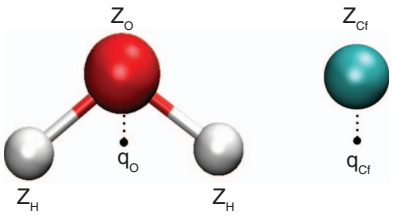

FIG. 1. Schematic representation of MCDHO model for the water molecule and the californium cation.

The improvements to the HIW model, on the basis of a flexible hydrated ion model[24,25] were:

- To take into account different hydrated ions $[Cf(H_2O)_n]^{3+}$] (where $n = 6$–10),
- To employ a flexible polarizable water model, the Mobile Charge Density Harmonic Oscillator model (MCDHO),[33]
- To define only one type of water molecule.

Now the possibility of water release between the first hydration shell and the bulk is permitted, as water molecule can change its polarization degree in a great extent, and differing from the previous model, there are not two types of water molecules (first-shell and bulk) defined in the system any more.

The monoatomic cation, Cf(III), is described by a positive charge, $Z_{Cf} = 4$, and a mobile negative charge density, ρ_{Cf} with a total charge, $q_{Cf} = -1$, joined to the nucleus by a spring of force constant, k_{Cf} (see Figure 1). The intra-atomic energy is defined by

$$U_{intra} = \frac{1}{2} k_{Cf} \cdot r^2, \tag{1}$$

where r is the distance between the nucleus and its associated mobile charge density. In the absence of an external field, the equilibrium position of the oscillator is located on the nucleus and $U_{intra} = 0$.

The incorporation of the MCDHO model to the new potential needs the consideration of the following intermolecular terms for the Cf(III)-H_2O interaction:

- Classical interaction between the mobile charge densities, q_O and q_{Cf}, given by a two-exponential function:

$$U_{inter}(q_O, q_{Cf}) = A_{CfO} \cdot e^{-\alpha_{CfO} \cdot r_{CfO}} + B_{CfO} \cdot e^{-\beta_{CfO} \cdot r_{CfO}}, \tag{2}$$

  where r_{CfO} is the distance between the mobile charge densities. A_{CfO}, α_{CfO}, B_{CfO}, and β_{CfO} are fitting parameters.
- Classical interaction between the Cf nucleus, Z_{Cf}, and those of the water molecule, Z_i ($i \equiv$ O, H), is given by a two-exponential function as well:

$$U_{inter}(Z_i, Z_{Cf}) = C_{Cfi} \cdot e^{-\gamma_{Cfi} \cdot R_i} + D_{Cfi} \cdot e^{-\delta_{Cfi} \cdot R_i}, \tag{3}$$

  where R_i is the distance between the Cf nucleus and each ith nucleus of the water molecule, and C_{Cfi}, γ_{Cfi}, D_{Cfi}, and δ_{Cfi} are fitting parameters.
- Electrostatic interaction between the water mobile charge density, q_O and the Cf nucleus, Z_{Cf}:

$$U_{inter}(q_O, Z_{Cf}) = \frac{q_O Z_{Cf}}{r'} \left[1 - \left(\frac{r'}{\lambda'} + 1 \right) e^{-2r'/\lambda'} \right], \tag{4}$$

  where r' is the distance between the center of ρ_O and the Cf nucleus and λ' is the intermolecular screening described in the original MCDHO model.[33]
- Electrostatic interaction between the Cf mobile charge density, q_{Cf}, and each of the charges on the water molecule nuclei, Z_i ($i \equiv$ O, H):

$$U_{inter}(Z_i, q_{Cf}) = \frac{Z_i q_{Cf}}{r_i} \left[1 - \left(\frac{r_i}{\lambda'_{Cf}} + 1 \right) e^{-2r_i/\lambda'_{Cf}} \right], \tag{5}$$

  where r_i is the distance from the ρ_{Cf} center to Z_i and λ'_{Cf} is the corresponding intermolecular screening.

Thus, the interaction energy for a cluster with N water molecules is computed by the expression

$$U = \sum_{S=1}^{N} \left(\sum_{i \in S} \sum_{j \in T} [U_{inter}(Z_i, Z_j) + U_{inter}(q_i, q_j) + U_{inter}(q_i, Z_j) + U_{inter}(q_j, Z_i)] + \sum_{i \in S} \frac{1}{2} k_i \cdot r_{ii}^2 + \frac{1}{2} k_{Cf} \cdot r^2 \right), \tag{6}$$

where S runs over the water molecules and T over the Cf.

It is worth commenting at this point that the set of structures chosen to be included in the fitting contain the fundamental ion-water interactions mediated by the presence of other water molecules either on the same shell or in a second shell. A wide range of distances and a number of water molecules are covered. Thus, the many-body ion-water interactions are implicitly included in the water interaction potential in a thorough way. Additionally, the flexible and polarizable character of the chosen water model guarantees the good behavior of perturbed water-water interactions of solvation shells beyond the second one.

B. Definition of the sets of structures

Two different methodologies have been used to select the set of structures to be fitted. The first one, which was used in our previous communication,[31] could be called "Heuristic method," as we adopted a practical iterative way of improving the interaction potential. The second one, developed in this work, has been defined by avoiding the iterative process, following a systematic choice of representative structures. It will be called "Systematic method."

1. Heuristic method (A)

1. Optimization of the hydrated cation for several coordination numbers, $[Cf(H_2O)_n]^{3+}$ (n = 6–9), and these hydrates solvated by several water molecules in their second hydration shell, $[Cf(H_2O)_n]^{3+})H_2O)_\ell$. (see Fig. 2).

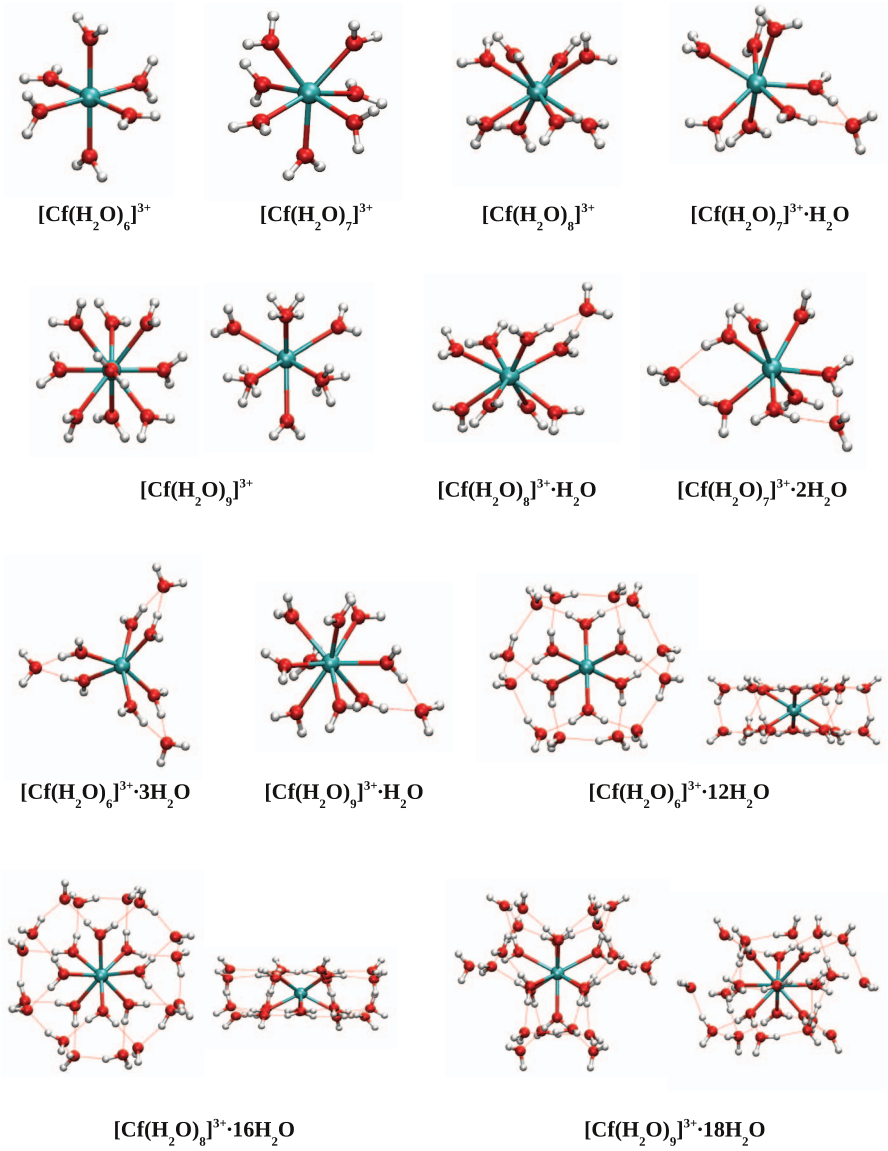

FIG. 2. QM-optimized structures for several californium clusters.

2. Taking as starting point the optimized structure of the Cf(III) octahydrate, one of its water molecules is moved along its Cf–O direction, scanning the Cf–O distance in the range 2.0–7.0 Å. From the optimized structure of the Cf(III) enneahydrate, we perform the scanning twice, one for an axial and another for an equatorial water molecule (see Fig. 3).
3. Steps 1 and 2 generate 200 geometries approximately. An iterative process such as sketched out in Fig. 4 is applied. The fitted potential is employed in a Monte Carlo simulation from which a set of structures is taken and their interaction energies compared to the QM values. If they are not reproduced by the potential, then they are incorporated to the structure set and a new fitting is carried out.

Two interaction potentials using this methodology (hereafter called **A**) were built. One is derived from the BP86 PES (hereafter called **a**) and the other from the MP2 PES (hereafter called **b**). Then **Pot_Aa** and **Pot_Ab** potentials are built after

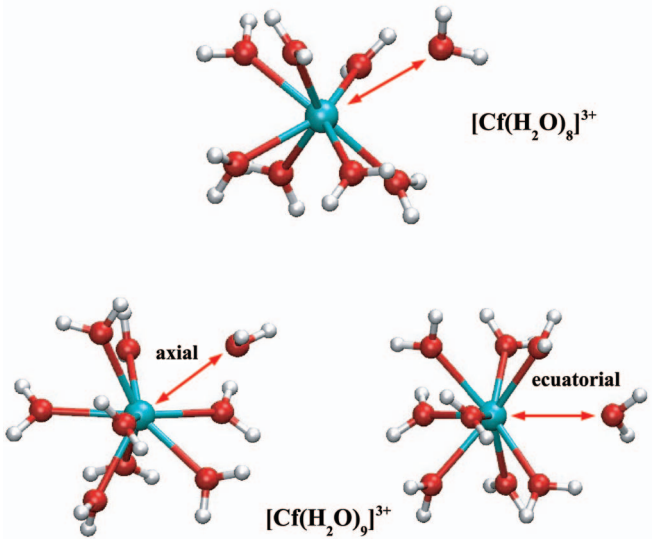

FIG. 3. Schematic representation of some structures employed in the development of the potentials.

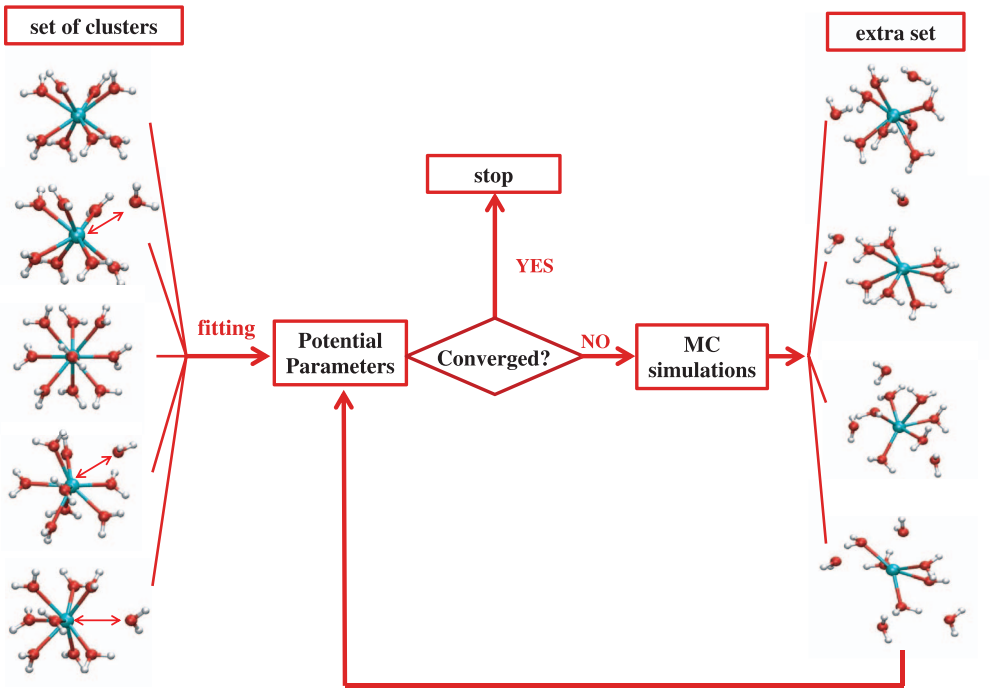

FIG. 4. Schematic representation of method A.

some iterations including in the final fitting a total number of structures of 1431 and 2849, respectively.

2. Systematic method (B)

Bearing in mind the application of this model to other actinoids, and other cations in general, a second method has been considered to establish a systematic way of generating an appropriate structure set:

1. Step 1 of method A.
2. Taking as starting point the optimized structure of the Cf(III) octahydrate, one of its water molecules is moved along its Cf–O direction, scanning the Cf–O distance in the range 2.0–7.0 Å, for nine evenly distributed orientations of the water molecule. The quaternion representation for the orientation was linked to the uniform distribution of nine points in an hyper-sphere.[34] Fig. 5(a) plots an example of the nine orientations for a given Cf–O distance. The same set of structures is generated for the two types of water molecules in the Cf(III) enneahydrate (not shown in Fig. 5).
3. From the optimized geometries of the cation plus its first and second hydration shells, $[Cf(H_2O)_6]^{3+} \cdot (H_2O)_{12}$, $[Cf(H_2O)_8]^{3+} \cdot (H_2O)_{16}$ and $[Cf(H_2O)_9]^{3+} \cdot (H_2O)_{18}$, several structures with only a few molecules of the second shell are included $[Cf(H_2O)_6]^{3+} \cdot (H_2O)_\ell$ (where $\ell = 0, 2, 3, 4$), $[Cf(H_2O)_8]^{3+} \cdot (H_2O)_\ell$ (where $\ell = 0, 1, 2$) and $[Cf(H_2O)_9]^{3+} \cdot (H_2O)_\ell$ (being $\ell = 0, 1$) (see Fig. 5(b)).
4. A set of structures following the normal mode deformations of the Cf(III) octa- and ennea-hydrate were taken into account as well (see Fig. 5(c)). The asymmetric information on the aqua ions supplied by these structures is relevant to reach a robust interaction potential.
5. The previous steps of the protocol supplied about 1800 points for the fitting. 200 of these points were structures having high enough repulsive interaction energies to be excluded from the fit.

   The resulting interaction potential was combined with the water MCDHO potential to carry out a MC simulation. 500 snapshots were extracted from this MC run, 250 of them corresponded to snapshots where the Cf first-hydration shell was formed by one Cf(III) plus eight water molecules, and the other 250 ones to Cf(III) plus nine water molecules. Their quantum mechanical energies were computed, and the ensemble of points were added to the structure set, which becomes formed by about 2100 points. The new fit obtained did not differ significantly from the previous one and was chosen as the final potential. Thus, two new potentials, **Pot_Ba** and **Pot_Bb**, were obtained. This methodology is denoted by the letter **B** and the quantum-mechanical method used to obtain the set of *ab initio* interaction energies is again labeled by **a** (BP86) and **b** (MP2).

The scan of potential energy surfaces for the different hydrated ion-water clusters was carried out at BP86[35,36] and MP2[37,38] levels using the Gaussian G03 program.[39] For O and H atoms the aug–cc–pVDZ[40,41] basis sets were chosen. For Cf(III), Relativistic Effective Core Potentials (RECPs) specifically developed for this oxidation state by the Stuttgart-Koln group (ECP87MWB[42]) and its associated QZ quality basis sets (ECP87MWB-AVQZ) were employed. This 5f-in-core-pseudopotential belongs to a set of quasi-relativistic pseudopotentials for trivalent actinide elements, An(III). The inclusion of the 5f shell into the pseudopotential prevents the complexity of quantum mechanical calculations associated to the great number of low-lying states derived from

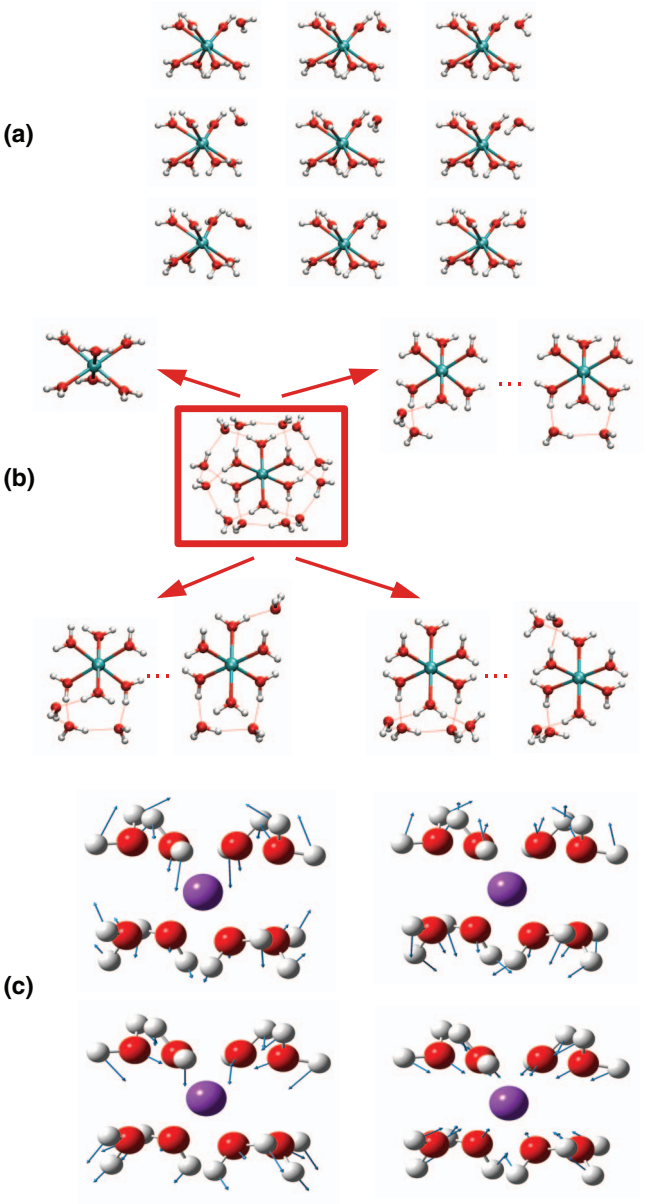

FIG. 5. Schematic representation of the different types of structures employed in the development of the potential using method B.

the $^{2S+1}$L term. The high oxidation state for which the 5f-in-core pseudopotential was developed together with the fact that Cf is a heavier actinide guarantees the core-like character of the 5f shell in this particular case. Previous studies including quantum mechanical calculations of the aqua ion series of actinoids support this assumption.[43]

Because of the large number of structures to be included in the fitting, it seems of interest to provide an idea about the computational cost of the quantum mechanical clusters. The whole set of single points of $[Cf(H_2O)_n]^{3+}$ clusters lasted about 40(BP86)–270(MP2) days of cpu-time/processor on an ALTIX-450 supercomputer, which in practice running parallel on this computer implies 2–14 wall-time days. Geometry optimizations of the different clusters took 70(BP86)–400(MP2) days of cpu-time/processor, which means 3.5–20 days.

TABLE I. Total and partial standard deviations (in kcal/mol) and numbers of structures associated to each of them.

	Pot_Aa	Pot_Ab	Pot_Ba	Pot_Bb
n_{tot}	1431	2849	2167	2117
σ_{tot}	6.76	5.46	3.58	6.11
n_1	881	2089	1384	1074
σ_1[a]	2.79	4.89	2.75	3.41
n_2	550	760	783	1043
σ_2[b]	11.59	5.32	5.15	7.56

[a]$\sigma_1 : E_{min} \le E \le (E_{min} + 60\,kcal/mol)$.
[b]$\sigma_2 : (E_{min} + 60\,kcal/mol) \le E \le E_{max}$.

C. Fitting procedure

The interaction energies were calculated as follow:

$$\Delta E_{int} = E_{[Cf(H_2O)_n]^{3+}} - E_{Cf^{3+}} - nE_{H_2O}, \quad (7)$$

and parameters in equation (6) were fitted to reproduce them.

The total number of geometries evaluated in the fitting procedure depended on both the quantum-mechanical PES and the method employed to build the intermolecular potential. Figure S1 of the supplementary material[54] shows a plot of fitted vs computed energies for the four potentials obtained. Their corresponding potential parameters are collected in Table S1 in the supplementary material. Standard deviations (SD) of the different fittings are summarized in Table I. In addition to the total SD for every fit, its distribution between the set of structures corresponding to the more attractive interactions ($E_{min} < E \le E_{min} + 60$ kcal/mol) and to the rest of selected points, ($E_{min} + 60$ kcal/mol $< E \le E_{max}$) has been included. It is seen that potentials give a better SD for the most attracting region which is in fact the most visited one during the statistical simulations.

III. RESULTS AND DISCUSSION

A. Minimizations

Numerical minimizations and Monte Carlo simulations were performed using the MCHANG program.[44]

In order to check the behavior of the new developed potentials, numerical minimizations of a set of representative structures were carried out. The selected structures included the Cf(III) hydrates, $[Cf(H_2O)n]^{3+}$ for $n = 1$–9, as well as the clusters with water molecules in the second hydration shell represented in Figure 2. The comparison among the clusters optimized by the classical intermolecular potentials and the quantum-mechanical methods is a test on the quality of the fitted potentials. In the supplementary material[54] Tables S2 and S3 collect the Cf–O distances obtained by using the four intermolecular potentials and the quantum-mechanical methods, BP86 and MP2. Their corresponding interaction energies are collected in Tables S4 and S5 in the supplementary material.[54] The standard deviations for both magnitudes have been collected in Table II.

The comparison of quantum and classical geometries for the smaller hydrated ions ($n = 1, 2, 4$) is not as good as for the aqua ions with larger hydration numbers. This may be understood on the fact that the small hydrates have not

TABLE II. Standard deviations for Cf–O distances and interaction energies for $[Cf(H_2O)_n]^{3+} \cdot (H_2O)_\ell$ clusters collected in Tables S1 and S2 in the supplementary material.[54]

Set of structures	Reference	Standard deviations	
		R_{Cf-O} (Å)	ΔE_{int} (kcal/mol)
Pot_Aa	BP86	0.11	15
Pot_Ba	BP86	0.06	12
Pot_Ab	MP2	0.04	9
Pot_Bb	MP2	0.03	11
BP86	MP2	0.03	27

been included in the fitting structure set. The general behavior is quite satisfactory for both distances and interaction energies (see Tables S2–S5 in the supplementary material[54]). The largest SD value for the structures is found for Pot_Aa and it is mainly due to the structure $[Cf(H_2O)_6]^{3+} \cdot (H_2O)_{12}$, where the second hydration shell appears to be too much distant from the hexahydrate. If these data are excluded, the standard deviation goes down to 0.09 Å. The resulting classical structures for the octa- and ennea-hydrated ion are in good agreement not only with our quantum optimized hydrated ion but also with previous quantum results published by Dolg *et al.*[43] (2.495 Å for the octahydrated and 2.537 Å for the enneahydrated ion). Moreover, when we consider the hydrated ion with its second solvation shell, the distance and orientation agreement is remarkable, as shown in Figure 6, where MP2 optimized structures are compared with those optimized with the Pot_Bb potential.

In that concerning the interaction energies, the SD values show the quality of the different fits, in particular bearing in mind that the average values for the interaction energies are −494 and −510 kcal/mol for BP86 and MP2, respectively.

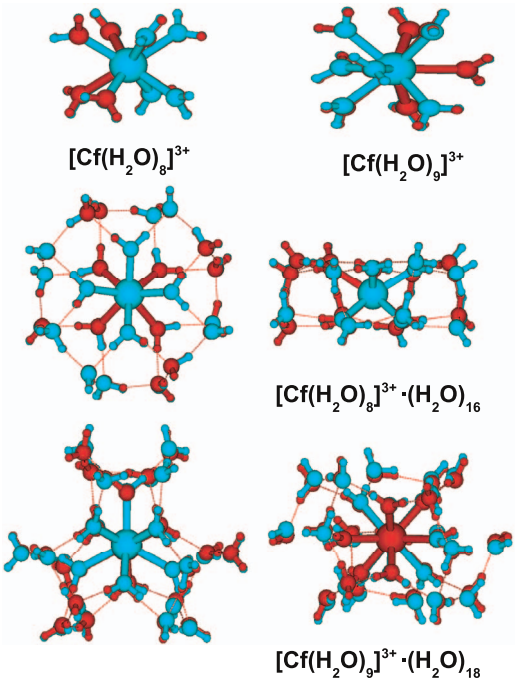

FIG. 6. Comparison between MP2 (QM) and Pot_Bb (MC) geometries.

For comparative purposes, Table II includes the SD associated to the structural and interaction energy comparison between both quantum mechanical methods, i.e., BP86 vs. MP2 results.

B. Monte Carlo simulations

Monte Carlo simulations were performed in the canonical ensemble (NVT) using the Monte Carlo-Metropolis[45] algorithm implemented in the MCHANG program.[44] Periodic boundary conditions[46] were applied and Ewald sum technique[46,47] was employed to calculate the electrostatic interactions. The system was formed by one Cf^{3+} and 500 water molecules in a cubic box of side length $L = 24.860$ Å. The new developed potentials were employed to describe the Cf-water interaction and the MCDHO potential[33] was used to describe the water-water interaction. Equilibration run of 10^9 configurations was carried out for each simulation preceding to the production runs.

1. Simulations performed using potentials derived from method A

Structures for analysis were taken from a statistical sampling of 10^9 configurations. The Radial Distribution Functions (RDFs) for Cf–O and Cf–H are shown in Figure 7(top). Hydration numbers and average Cf–O and Cf–H distances were also extracted and summarized in Table III.

The MC simulation using the Pot_Aa potential leads to an average coordination number for the first solvation shell close to 7.5, the Cf–O distance for this first-shell appears at 2.43 Å, whereas the MC simulation which uses the Pot_Ab potential gives a larger hydration number, 8.6, and a longer Cf–O distance of 2.54 Å. The second hydration shell is formed by 18 (Pot_Aa simulation) and 19 (Pot_Ab simulation) water molecules at an average distance of 4.65 and 4.70 Å, respectively. Cf–H RDFs show the peaks corresponding to the first and second hydration shell shifted by about 0.6–0.7 Å with respect to the Cf–O peaks. This indicates that an ion-dipole orientation is adopted by these water molecules, as expected for the high charge of the cation.

2. Simulations performed using potentials derived from method B

Structures for analysis were taken from a statistical sampling of 4×10^9 configurations. Cf–O and Cf–H RDFs are shown in Figure 7 (bottom). Hydration numbers and Cf–O and Cf–H distances are collected in Table III.

Both simulations lead to a first-shell coordination number close to 8 (Pot_Ba:7.8 and Pot_Bb:8.0). The first-shell Cf–O distances are 2.47 and 2.48 Å, respectively. The second hydration shell is formed by ∼19 (Pot_Ba) and ∼18 (Pot_Bb) water molecules at average distances of 4.69 and 4.72 Å, respectively. The shifted peaks of Cf–H RDFs with respect to the Cf–O ones, also support the ion-dipole orientation adopted by water molecules in the second shells. Spezia *et al.*[15] from MD simulations give three Cf–O estimations for the first shell, in

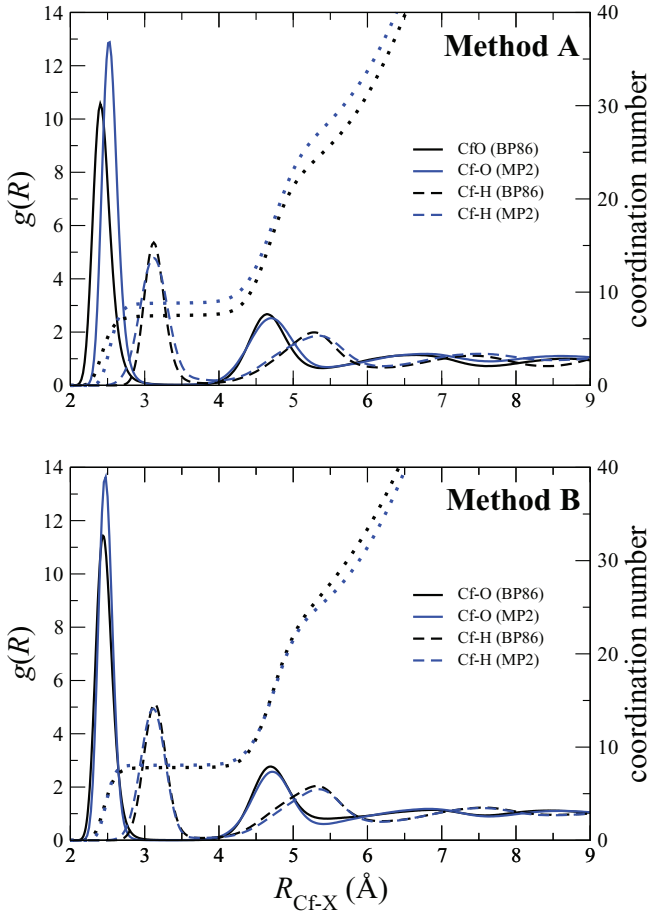

FIG. 7. Cf–O and Cf–H radial distribution functions (RDFs) and their corresponding running integration numbers (dotted lines) derived from the different MC simulations.

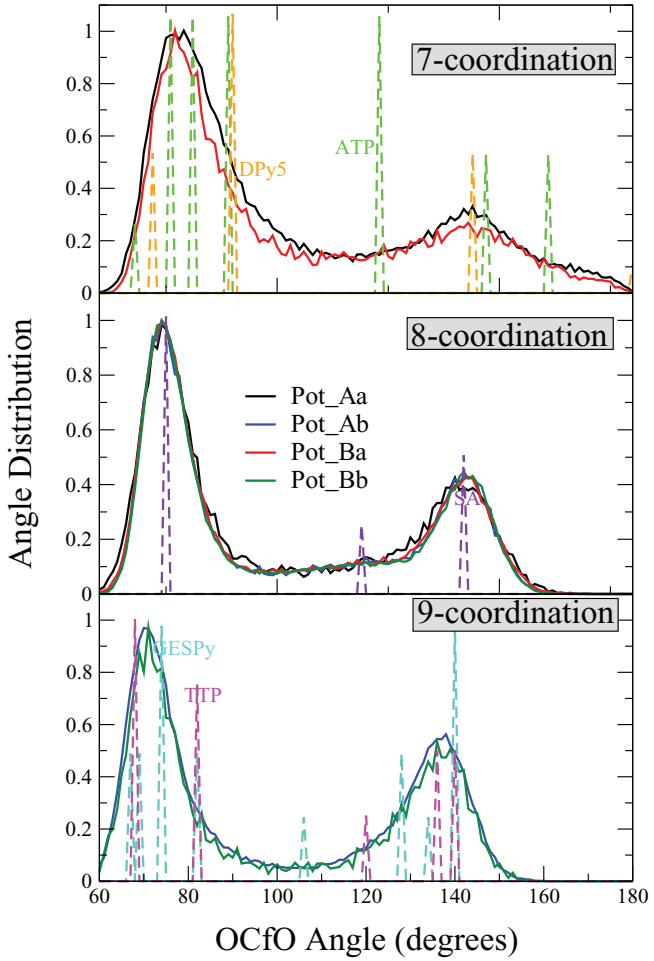

FIG. 8. O–Cf–O angle distribution functions (ADFs) derived from the different MC simulations, for the 7-, 8-, and 9- coordination. The delta functions correspond to the more similar distributions of ideal polyhedra of the different N-coordination: for N = 7: Augmented Triangular Prims (ATP) and Dipyramid pentagonal (DPy5); for N = 8: Square Antiprism (SA); for N = 9: Trigonal Tricapped Prism (TTP) and Gyro-elongated Square Pyramid (GESPy).

the range 2.39–2.44 Å, assuming three possible coordination numbers, 8, 8.5, and 9. For the second-shell Cf–O distance the values found are in the range, 4.56–4.62 Å.

In addition to the site-site pairwise information provided by the RDFs, the three-body information given by the O–Cf–O angle distribution is valuable to get insight into the type of geometry adopted by the hydrated ion for a given coordination.[14–16,48] The comparison of the angle distribution function (ADF) extracted from the simulation with the distribution exhibited by an ideal polyhedron may be useful to identify an average symmetry for the aqua ion in solution.

TABLE III. Cf–O and Cf–H distances and hydration numbers corresponding to the first and second hydration shells.

Potential	Pair	R_1 (Å)	n_1	R_2 (Å)	n_2
Pot_Aa	Cf–O	2.43	7.5	4.65	18
	Cf–H	3.14	15.0	5.28	49
Pot_Ab	Cf–O	2.54	8.6	4.70	19
	Cf–H	3.15	18.8	5.35	53
Pot_Ba	Cf–O	2.47	7.8	4.69	19
	Cf–H	3.15	16.4	5.31	57
Pot_Bb	Cf–O	2.48	8.0	4.72	18
	Cf–H	3.11	19.6	5.34	57

Figure 8 plots the ADFs for the different coordination numbers together with the distributions corresponding to the most similar ideal polyhedron. For clarity reasons, Figure 8 has been split into three plots, which correspond to the three coordination numbers observed along the simulations for each potential. Given that the different interaction potentials lead to different coordination numbers (see Table III), there is not a significant number of structures of the 7-coordination for simulations with Pot_Ab and Pot_Bb. The 9-coordination is almost absent for the cases of Pot_Aa and Pot_Ba.

The first interesting result is that for a given N-coordination the ADF is the same regardless the potential employed in the simulation. This means that the water molecule distribution around Cf(III) follows the same pattern, even though the effective pair-interaction potentials were as different as leading to hydration number values differing in more than one unit. Regarding the preferred symmetry, Figure 8 includes only the delta ideal polyhedron ADFs corresponding to the most similar distributions to the simulation ADFs. Thus, 8-coordination ADFs resemble the ideal distribution

corresponding to a Square Antiprism (SA), as suggested by several authors who had previously examined other octa-coordinated aqua ions of lanthanoids and actinoids.[14–16,48] For the 9-coordination the direct comparison of ideal polyhedra delta functions and the simulation ADFs cannot give an unambiguous answer on either Tricapped Trigonal Prism (TTP) or Gyroelongated Square Pyramid (GESPy) is the preferred coordination. Other authors have suggested that TTP is the preferred one,[14,15,48] although as claimed by Atta-Fynn *et al.*[14] when studying the Cm(III) aqua ion, the strong thermal effects and the intrinsic dynamics of the liquid medium make difficult a simple comparison between the distorted structures of the aquaion in solution and the ideal crystal unit. Further insights are needed on this issue. When dealing with the 7-coordination, the comparison leads to a situation similar to that of the 9-coordination, i.e., the Augmented Triangular Prism (ATP) and the Dipyramid5 (DPy5) ideal polyhedra are close to ADFs obtained from simulations, provided that significant distribution broadening should occur in angular regions close to 90°, 120°, and 160° when passing from the ideal crystal to solution.

C. EXAFS spectrum simulation

As mentioned in the Introduction, among the very scarce experimental information on Cf(III) in solution, X-ray absorption spectroscopy is one of the experimental techniques giving structural information.[2,31,49] In our previous communication,[31] it was shown that the comparison between the k^2-weighted experimental EXAFS spectrum of an 1mM Cf(III) aqueous solution and that theoretically computed from the MC simulations could shed light on the structural elucidation of Cf(III) hydration. 500 configurations taken from each MC simulation have been used to compute individually the EXAFS spectrum by using the FEFF code (v.8.4) developed by Rehr *et al.*[50,51] The average spectrum obtained from each simulation is plotted in Figure 9 (method A (top), method B (bottom)). Details of the procedure employed to simulate the spectra can be found elsewhere.[29,31,52] A typical input FEFF file has also been included in the supplementary material[54] for details on the spectrum computation conditions. It is worth pointing out that the comparison among the experimental and theoretical results is based on the EXAFS spectrum in the *k*-space. This means that no aprioristic preferred Cf hydrate has been introduced in the structural analysis, as usually is done by Fourier Transform leading to the EXAFS spectrum in the *R*-space, when a standard experimental EXAFS fit is carried out.

Using two Cf–O cutoffs to select the number of hydration shells around the Cf(III) cation, it has been shown that the second hydration shell does not contribute significantly to the computed EXAFS signal.

The simulated EXAFS spectra derived from method A, Pot_Aa and Pot_Ab, differ in both the frequency and the intensity of the signal. The first one reflects the gap of ~0.1 Å exhibited by $R_{\mathrm{Cf-O_I}}$ (2.43 Å for Pot_Aa and 2.54 Å for Pot_Ab), as may also be checked examining the first peak in Cf–O RDFs in Figure 7(top). The second one runs parallel to the structural and dynamical disorder which may be quantified by the Debye-Waller (DW) factor. The value corresponding to the first-shell Cf–O contribution can be computed as the second-order cumulant of $R_{\mathrm{Cf-O_I}}$ distribution[52,53]

$$\sigma^2_{\mathrm{Cf-O_I}} = \langle (\mathrm{R}_{\mathrm{Cf-O_I}} - \overline{R}_{\mathrm{Cf-O_I}})^2 \rangle. \quad (8)$$

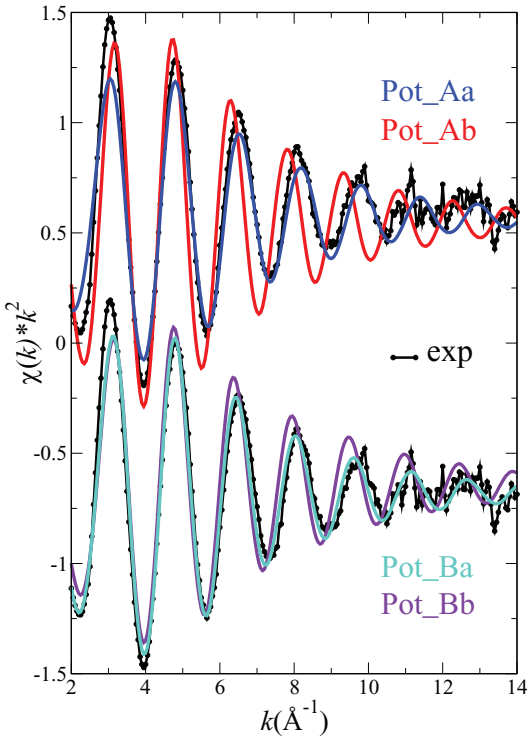

FIG. 9. Comparison of the experimental EXAFS spectrum for Cd(III) with the computed spectra obtained from the set of snapshots of the MC simulations using Pot_Ba and Pot_ Bb potentials.

DW factor is larger for Pot_Aa ($\sigma^2_{\mathrm{Cf-O_I}} = 0.013$ Å^2) than for Pot_Ab ($\sigma^2_{\mathrm{Cf-O_I}} = 0.009$ Å^2), and its average coordination number is smaller in one unit (7.5 vs 8.6 for Pot_Aa and Pot_Ab, respectively). Both factors favor a signal intensity lower in the Pot_Aa simulated EXAFS spectrum than in the Pot_Ab one. The Pot_Aa spectrum is more similar to the experimental one than the spectrum derived from the Pot_Ab simulation. The spectra derived from the application of method B are mutually more similar than those of method A, in particular in the frequency of the signal. The difference in the signal intensity comes from the gap in the DW factor value which is smaller for Pot_Bb (0.006 Å^2) than for Pot_Ba (0.011 Å^2), since the first-shell coordination number is almost the same in both simulations (~8 in Table III). The comparison with the experimental spectrum supports a better agreement with the Pot_Ba simulated spectrum. If we examine the slight differences between the simulated and experimental spectra around 8–9 Å^{-1}, it is noticeable how the Aa and Ba simulations delimit the experimental signal. Thus, these data extracted from both MC simulations suggest that the experimental Cf−O$_I$ distance should be between 2.43 and 2.47 Å, with an average hydration number of 8, and a DW factor value of about 0.012 Å^2. D'Angelo *et al.*[22] have worked out the same EXAFS spectrum on two different models of coordination number, obtaining a Cf–O

distance range of 2.37–2.49 Å for a TTP geometry or 2.42 Å for a symmetric ennea-coordination, together with a DW factor of 0.007–0.008 $Å^2$.

IV. CONCLUDING REMARKS

This work has established a new method of interaction potential building between highly charged metal cations and water to be used in classical computer simulations. No empirical parameters are included in the development, the interaction potential has been fitted to reproduce quantum-mechanical information derived from a wide set of $[Cf(H_2O)_n]^{3+} \cdot (H_2O)_\ell$ clusters. The extension of our primitive hydrated ion-water model (HIW),[9,25,26] that allowed us to collect a significant part of the many-body contributions, has been based on the combined use of a polarizable and flexible water model, the MCDHO one,[33] and the selection of a set of ion-water structures for the building potential with a representative number of water molecules (6–27). This has overtaken the previous limitation of first-shell water exchange with outer hydration shells. This is the reason we propose to call "Exchange-HIW potential" to this new type of interaction potential.

It has been shown the quality of potentials by performing numerical minimizations for the hydrated ions with its first and second solvation shells and their comparison with results from the two quantum levels considered (DFT and MP2). The application of the Systematic method (B) for the potential building has shown that there is not a significant conflict between the BP86 and MP2 quantum-mechanical methods, as seemed to rise in our previous communication,[31] in predicting a given coordination number. It is rather a subtle question associated to the $[Cf(H_2O)_m]^{3+} (H_2O)_\ell$ cluster choosing way, which appears to present a large sensitivity to the ion-water coordination.

From the comparison among experimental and computed EXAFS spectra it has been shown that the preferred hydration number is 8. The use of potentials derived from the Systematic methodology confirms the initial results, and allows the proposal of a $Cf-O_I$ average distance in the range 2.43–2.47 Å. The agreement is particularly noticeable for the signal intensity between the simulated EXAFS spectrum derived from Pot_Ba and the experimental spectrum. There is also a good description of the structural fluctuation and dynamic disorder, which can be quantified by a DW value of ∼0.010 $Å^2$ for the $Cf-O_I$ paths. Analysis of OCfO angle distributions shows that these are common for a given coordination number, regardless the intermolecular potential employed. For the 8-coordinated clusters in solution, distributions suggest a square antiprism polyhedron.

The combination of experimental X-ray absorption spectroscopy and computer simulations allows us a quite confident assignment of the coordination number and the metal-oxygen distance. Beyond this particular case of Cf(III), a systematic theoretical and experimental examination on other experimentally known actinoids treated on the same manner must be performed to get insight into the trend along the series, as it has already been initiated by other authors.[15,22]

ACKNOWLEDGMENTS

Spanish Ministry of Science and Innovation is acknowledged for financial support (CTQ2011-25932).

[1] R. J. Silva and H. Nitsche, Radiochim. Acta **70–71**, 377 (1995).
[2] M. A. Denecke, Coord. Chem. Rev. **250**, 730 (2006).
[3] L. Soderholm and M. Antonio, *The Chemistry of the Actinide and Transactinide Elements*, 3rd ed. (Springer, Dordrecht, 2006), pp. 3086–3198.
[4] D. Marx and J. Hutter, *Ab Initio Molecular Dynamics: Basic Theory and Advanced Methods* (Cambridge University Press, Cambridge, 2009).
[5] A. J. Stone, *The Theory of Intermolecular Forces*, 2nd ed. (Oxford University Press, Oxford, 2013).
[6] F. M. Floris and A. Tani, *Molecular Dynamics. From Classical to Quantum Methods* (Elsevier, Amsterdam, 1999), Chap. 10.
[7] P. M. Balbuena, L. Wang, T. Li, and P. A. Derosa, *Molecular Dynamics. From Classical to Quantum Methods* (Elsevier, Amsterdam, 1999), Chap. 11.
[8] T. Yang and B. E. Bursten, Inorg. Chem. **45**, 5291 (2006).
[9] R. R. Pappalardo and E. Sánchez Marcos, J. Phys. Chem. **97**, 4500 (1993).
[10] R. R. Pappalardo, J. M. Martínez, and E. Sánchez Marcos, J. Phys. Chem. **100**, 11748 (1996).
[11] J. M. Martínez, R. R. Pappalardo, E. Sánchez Marcos, K. Refson, S. Díaz-Moreno, and A. Muñoz-Paez, J. Phys. Chem. B **102**, 3272 (1998).
[12] D. Hagberg, E. Bednarz, N. M. Edelstein, and L. Gagliardi, J. Am. Chem. Soc. **129**, 14136 (2007).
[13] O. Engkvist, P. Åstrand, and G. Karlström, Chem. Rev. **100**, 4087 (2000).
[14] R. Atta-Fynn, E. J. Bylaska, G. Schenter, and W. de Jong, J. Phys. Chem. A **115**, 4665 (2011).
[15] M. Duvali, F. Martelli, P. Vitorge, and R. Spezia, J. Chem. Phys. **135**, 044503 (2011).
[16] M. Duvail, P. Vitorge, and R. Spezia, J. Chem. Phys. **130**, 104501 (2009).
[17] M. Duvail, M. Souaille, R. Spezia, T. Cartailler, and P. Vitorge, J. Chem. Phys. **127**, 034503 (2007).
[18] B. M. Rode, T. S. Hofer, B. R. Randolf, C. F. Schwenk, D. Xenides, and V. Vchirawongkwin, Theor. Chem. Acc. **115**, 77 (2006).
[19] R. J. Frick, A. B. Pribil, T. S. Hofer, B. R. Randolf, A. Bhattacharjee, and B. M. Rode, Inorg. Chem. **48**, 3993 (2009).
[20] F. H. David and B. Fourest, New J. Chem. **21**, 167 (1997).
[21] P. G. Allen, J. Bucher, D. Shuh, N. Edelstein, and I. Carig, Inorg. Chem. **39**, 595 (2000).
[22] P. D'Angelo, F. Martelli, R. Spezia, A. Filipponi, and M. A. Denecke, Inorg. Chem. **52**, 10318 (2013).
[23] C. Apostolidis, B. Schimmelpfennig, N. Magnani, P. Lindqvist-Reis, O. Walter, R. Sykora, A. Morgenstern, E. Colineau, R. Caciuffo, R. Klenze, R. Haire, J. Rebizant, F. Bruchertseifer, and T. Fanghänel, Angew. Chem. Int. Ed. **49**, 6343 (2010).
[24] J. M. Martínez, R. R. Pappalardo, and E. Sánchez Marcos, J. Chem. Phys. **109**, 1445 (1998).
[25] J. M. Martínez, R. R. Pappalardo, and E. Sánchez Marcos, J. Am. Chem. Soc. **121**, 3175 (1999).
[26] J. M. Martínez, F. Torrico, R. R. Pappalardo, and E. Sánchez Marcos, J. Phys. Chem. B **108**, 15851 (2004).
[27] J. M. Martínez, P. J. Merkling, R. R. Pappalardo, K. Refson, and E. Sánchez Marcos, Theor. Chem. Acc. **111**, 101 (2004).
[28] F. Torrico, R. R. Pappalardo, E. Sánchez Marcos, and J. M. Martínez, Theor. Chem. Acc. **115**, 196 (2006).
[29] F. Carrera, F. Torrico, D. T. Richens, A. Muñoz-Páez, J. M. Martínez, R. R. Pappalardo, and E. Sánchez Marcos, J. Phys. Chem. B **111**, 8223 (2007).
[30] L. Helm and A. E. Merbach, Chem. Rev. **105**, 1923 (2005).
[31] E. Galbis, J. Hernández-Cobos, C. Den Auwer, C. Le Naour, D. Guillaumont, E. Simoni, R. R. Pappalardo, and E. Sánchez Marcos, Angew. Chem. Int. Ed. **49**, 3811 (2010).
[32] E. Sánchez Marcos, R. R. Pappalardo, J. C. Barthelat, and F. X. Gadea, J. Phys. Chem. **96**, 516 (1992).
[33] H. Saint-Martin, J. Hernández-Cobos, M. I. Bernal-Uruchurtu, I. Ortega-Blake, and H. J. C. Berendsen, J. Chem. Phys. **113**, 10899 (2000).
[34] E. L. Altschuler and A. Pérez-Garrido, Phys. Rev. E **76**, 016705 (2007).
[35] A. D. Becke, Phys. Rev. A **38**, 3098 (1988).
[36] J. P. Perdew, Phys. Rev. B **33**, 8822 (1986).

[37]C. Møller and M. S. Plesset, Phys. Rev. **46**, 618 (1934).
[38]I. L. Alberts and N. C. Handy, J. Chem. Phys. **89**, 2107 (1988).
[39]M. J. Frisch, G. W. Trucks, H. B. Schlegel *et al.*, Gaussian 03, Revision C.02, Gaussian, Inc., Wallingford, CT, 2004.
[40]T. H. J. Dunning, J. Chem. Phys. **90**, 1007 (1989).
[41]R. A. Kendall, T. H. J. Dunning, and R. J. Harrison, J. Chem. Phys. **96**, 6796 (1992).
[42]A. Moritz, X. Cao, and M. Dolg, Theor. Chem. Acc. **117**, 473 (2007).
[43]J. Wiebke, A. Moritz, X. Cao, and M. Dolg, Phys. Chem. Chem. Phys. **9**, 459 (2007).
[44]"Mchang," MCHANG program is available upon request at jorge@fis.unam.mx.
[45]N. Metropolis, A. W. Rosenbluth, M. N. Rosenbluth, A. H. Teller, and E. Teller, J. Chem. Phys. **21**, 1087 (1953).
[46]M. P. Allen and D. J. Tildesley, *Computer Simulation of Liquids* (Oxford University Press, New York, 1987).
[47]P. P. Ewald, Ann. Phys. **369**, 253 (1921).
[48]T. Kowall, F. Foglia, L. Helm, and A. E. Merbach, J. Phys. Chem. **99**, 13078 (1995).
[49]R. Revel, C. den Auwer, C. Madic, F. David, B. Fourest, S. Hubert, J.-F. Le Du, and L. R. Mors, Inorg. Chem. **38**, 4139 (1999).
[50]J. J. Rehr and R. C. Albers, Rev. Mod. Phys. **72**, 621 (2000).
[51]A. L. Ankudinov, A. I. Nesvizhskii, and J. J. Rehr, Phys. Rev. B **67**, 115120 (2003).
[52]P. J. Merkling, A. Muñoz-Páez, and E. Sánchez Marcos, J. Am. Chem. Soc. **124**, 10911 (2002).
[53]L. Campbell, J. Rehr, G. Schenter, M. McCarthy, and D. Dixon, J. Synchrotron Radiat. **6**, 310 (1999).
[54]See supplementary material at http://dx.doi.org/10.1063/1.4879549 for Figure S1 showing the quality of the fits of the different intermolecular potentials, Table S1 giving the potential parameters, Tables S2–S5 comparing distances and interactions energies obtained from quantum-mechanical and interaction potentials, and two FEFF input files used for the EXAFS spectrum simulation.